arXiv:nlin/0302031v1 [nlin.SI] 13 Feb 2003

Renormalization Group Reduction of the Henon Map and Application to the Transverse Betatron Motion in Cyclic Accelerators*

Stephan I. Tzenov and Ronald C. Davidson
Plasma Physics Laboratory, Princeton University, Princeton, New Jersey, 08543

Abstract

The renormalization group method is applied to the study of discrete dynamical systems. As a particular example, the Henon map is considered as applied to describe the transverse betatron oscillations in a cyclic accelerator or storage ring possessing a FODO-cell structure with a single thin sextupole. A powerful renormalization group method is developed that is valid correct to fourth order in the perturbation amplitude, and a technique for resolving the resonance structure of the Henon map is also presented. This calculation represents the first successful application of a renormalization group method to the study of discrete dynamical system in a unified manner capable of reducing the dynamics of the system both far from and close to resonances, thus preserving the symplectic symmetry of the original map.

*Supported by U.S. Department of Energy contract DE-AC02-76CH03073.

1 Introduction and Basic Equations

It is increasingly important to develop an improved theoretical understanding of the nonlinear dynamics of charged particle beams in high energy accelerators and storage rings [1, 2, 3, 4, 5, 6]. An individual particle propagating in an accelerator experiences a growth of amplitude of betatron oscillations in a plane transverse to the particle orbit whenever a perturbing force acts on it. This force may be of various origins, for example, high-order multipole magnetic field errors, space-charge forces, beam-beam interaction force, power supply ripples, or other external and collective forces.

There is a growing number of robust analytical methods used to study the effects of the nonlinear behavior of beams in accelerators and storage rings, ranging from classical perturbation theory [7, 8] to the Lie algebraic approach [9, 10, 11]. The recently developed renormalization group (RG) method has been successfully applied to both continuous dynamical systems [12, 13, 14] and maps [15, 16] that are of general interest in the physics of accelerators and beams. The advantage of the RG method is associated with the fact that it is equally powerful to study finite-dimensional, as well as continuous systems. Therefore, it is also useful when applied to analyze the properties of chaotic dynamical systems in both the stability region and the globally stochastic region in phase space [17, 18, 19].

While the RG method is well established in applications to continuous dynamical systems, the present paper demonstrates that the RG method can also be applied successfully to study discrete dynamical systems. As a particular example, we consider the Henon map [20, 21] as applied to describe the transverse betatron oscillations in a cyclic accelerator or storage ring possessing a FODO-cell structure with a single thin sextupole. The basic equations and Henon transfer map used in the present analysis are summarized later in section 1, and in section 2 a powerful RG technique is developed that is valid correct to fourth order in the perturbation amplitude. A technique for resolving the resonance structure of the Henon map is discussed in section 3, and in section 4 illustrative numerical results are presented.

The present analysis assumes that a certain multipole nonlinearity is concentrated at a single point azimuthally located at θ_0. Then the one-turn transfer map describing the transverse betatron motion in a cyclic accelerator or storage ring can be written in the form [22]

$$\mathbf{z}_{n+1} = \widehat{\mathcal{R}}_t \left[\mathbf{z}_n + \frac{l}{R} \mathbf{F}(\mathbf{z}_n; \theta_0) \right], \tag{1.1}$$

where $\mathbf{z}$ is the state vector

$$\mathbf{z} = \begin{pmatrix} X \\ P_x \\ Z \\ P_z \end{pmatrix}, \tag{1.2}$$

$\widehat{\mathcal{R}}_t$ is an orthogonal matrix

$$\widehat{\mathcal{R}}_t = \begin{pmatrix} \cos 2\pi\nu_x & \sin 2\pi\nu_x & 0 & 0 \\ -\sin 2\pi\nu_x & \cos 2\pi\nu_x & 0 & 0 \\ 0 & 0 & \cos 2\pi\nu_z & \sin 2\pi\nu_z \\ 0 & 0 & -\sin 2\pi\nu_z & \cos 2\pi\nu_z \end{pmatrix}, \tag{1.3}$$

and $\mathbf{F}(\mathbf{z};\theta_0)$ is defined by

$$\mathbf{F}(\mathbf{z};\theta_0) = \begin{pmatrix} 0 \\ -\dfrac{\partial V(X,Z;\theta_0)}{\partial X} \\ 0 \\ -\dfrac{\partial V(X,Z;\theta_0)}{\partial Z} \end{pmatrix}. \tag{1.4}$$

Here, (X, Z) is the transverse displacement, (P_x, P_z) is the transverse canonical momentum, l is the length of the multipole element, R is the mean machine radius and $\nu_{x,z}$ are the horizontal and the vertical betatron tunes, respectively. Furthermore, $V(X, Z;\theta)$ is the nonlinear potential, which can be expressed in the polynomial form

$$V(X,Z;\theta) = \sum_{I=2}^{\infty} \sum_{\substack{k,m=0 \\ k+m=I}}^{I} b_{km}^{(I)}(\theta) X^k Z^m, \tag{1.5}$$

where $b_{km}^{(I)}(\theta)$ are coefficients (generally functions of the azimuthal angle θ) representing the strength of the nonlinearity.

2 The Henon Map

The simplest nontrivial example of a polynomial transfer map is the so-called Henon map [20, 21]. It can describe the horizontal betatron oscillations in an accelerator possessing a FODO-cell structure with a single thin sextupole. The two-dimensional Henon map can be obtained from equation (1.1) in the case when the potential $V(X, Z;\theta)$ [see equation (1.5)] contains a single localized cubic nonlinearity. In explicit form it can be written as

$$X_{n+1} = X_n \cos\omega + \left(P_n - \mathcal{S}X_n^2\right)\sin\omega, \tag{2.1}$$

$$P_{n+1} = -X_n \sin\omega + \left(P_n - \mathcal{S}X_n^2\right)\cos\omega, \tag{2.2}$$

where

$$\omega = 2\pi\nu, \qquad \mathcal{S} = \frac{l\lambda_0(\theta_0)\beta^{3/2}(\theta_0)}{2R^3}. \tag{2.3}$$

In section 1, we briefly discussed the essence of the RG method and emphasized its power to handle a number of problems arising in the theory of continuous dynamical systems. In this section, we will demonstrate that the RG method can be applied successfully to study discrete dynamical systems, and as a particular example, we consider the Henon map. The latter can be further simplified by eliminating the canonical momentum variable P. Multiplying equation (2.1) by $\cos\omega$, multiplying equation (2.2) by $-\sin\omega$, and summing the two equations, we obtain

$$X_{n+1}\cos\omega - P_{n+1}\sin\omega = X_n. \tag{2.4}$$

Substitution of the recursion relation (2.4) into equation (2.1) yields the second-order difference equation for X

$$\widehat{\mathcal{L}}X_n = X_{n+1} - 2X_n\cos\omega + X_{n-1} = -\epsilon\mathcal{S}X_n^2\sin\omega. \tag{2.5}$$

Here, ϵ is a formal small parameter introduced for convenience to take into account the perturbative character of the sextupole nonlinearity.

Next we consider an asymptotic solution of the map (2.5) for small ϵ by means of the RG method. The naive perturbation expansion

$$X_n = X_n^{(0)} + \epsilon X_n^{(1)} + \epsilon^2 X_n^{(2)} + \ldots, \tag{2.6}$$

when substituted into equation (2.5), yields the perturbation equations order by order

$$\widehat{\mathcal{L}}X_n^{(0)} = 0, \tag{2.7}$$

$$\widehat{\mathcal{L}}X_n^{(1)} = -\mathcal{S}X_n^{(0)\mathbf{2}}\sin\omega, \tag{2.8}$$

$$\widehat{\mathcal{L}}X_n^{(2)} = -2\mathcal{S}X_n^{(0)}X_n^{(1)}\sin\omega, \tag{2.9}$$

$$\widehat{\mathcal{L}}X_n^{(3)} = -\mathcal{S}\Big(X_n^{(1)\mathbf{2}} + 2X_n^{(0)}X_n^{(2)}\Big)\sin\omega, \tag{2.10}$$

$$\widehat{\mathcal{L}}X_n^{(4)} = -2\mathcal{S}\Big(X_n^{(0)}X_n^{(3)} + X_n^{(1)}X_n^{(2)}\Big)\sin\omega. \tag{2.11}$$

Solving equation (2.7) for the zeroth-order contribution, we obtain the simple result

$$X_n^{(0)} = Ae^{i\omega n} + c.c., \qquad\qquad P_n^{(0)} = iAe^{i\omega n} + c.c., \tag{2.12}$$

where A is a complex constant amplitude. By virtue of equation (2.12) the first-order perturbation equation (2.8) becomes

$$\widehat{\mathcal{L}}X_n^{(1)} = -\mathcal{S}\Big(A^2e^{2i\omega n} + 2|A|^2 + c.c.\Big)\sin\omega. \tag{2.13}$$

The solution to equation (2.13) can be expressed as

$$X_n^{(1)} = -\mathcal{S}|A|^2\cot\frac{\omega}{2} + \frac{\sin\omega}{2}\mathcal{S}_1A^2e^{2i\omega n} + c.c., \tag{2.14}$$

where

$$\mathcal{S}_1 = \frac{\mathcal{S}}{\cos\omega - \cos 2\omega}. \tag{2.15}$$

To avoid resonant secular terms, we assume in addition that

$$\omega \neq 2k\pi, \qquad\qquad \omega \neq \frac{2\pi}{3} + 2k\pi, \qquad\qquad \omega \neq \frac{4\pi}{3} + 2k\pi, \tag{2.16}$$

where k is an integer. The properties of the Henon map in the case where the betatron tune is near a resonance (in particular the 1/3 resonance) will be considered in the section 3.

The second-order perturbation equation (2.9) becomes

$$\widehat{\mathcal{L}}X_n^{(2)} = -2\mathcal{F}\sin\omega|A|^2Ae^{i\omega n} - \sin^2\omega\mathcal{S}\mathcal{S}_1A^3e^{3i\omega n} + c.c., \tag{2.17}$$

where

$$\mathcal{F} = \mathcal{S}\Big(\frac{\mathcal{S}_1}{2}\sin\omega - \mathcal{S}\cot\frac{\omega}{2}\Big). \tag{2.18}$$

The solution to equation (2.17) can be readily expressed in the form

$$X_n^{(2)} = in\mathcal{F}|A|^2Ae^{i\omega n} + \frac{\sin^2\omega}{2}\mathcal{S}_1\mathcal{S}_2A^3e^{3i\omega n} + c.c., \tag{2.19}$$

where

$$\mathcal{S}_2 = \frac{\mathcal{S}}{\cos\omega - \cos 3\omega}, \qquad \omega \neq (2k+1)\pi, \qquad \omega \neq (2k+1)\frac{\pi}{2}. \tag{2.20}$$

Continuing further with the third-order calculation, we note that

$$\widehat{\mathcal{L}}X_n^{(3)} = -\mathcal{S}\Big(\Sigma_0|A|^4 + \Sigma_2|A|^2A^2e^{2i\omega n} + \Sigma_4A^4e^{4i\omega n} + c.c.\Big)\sin\omega. \tag{2.21}$$

Here, the notation

$$\Sigma_0 = \mathcal{S}^2\cot^2\frac{\omega}{2} + \frac{\mathcal{S}_1^2}{2}\sin^2\omega, \tag{2.22}$$

$$\Sigma_2 = \mathcal{S}_1\Big(\mathcal{S}_2\sin\omega - \mathcal{S}\cot\frac{\omega}{2}\Big)\sin\omega + 2in\mathcal{F}, \tag{2.23}$$

$$\Sigma_4 = \frac{\mathcal{S}_1}{4}(\mathcal{S}_1 + 4\mathcal{S}_2)\sin^2\omega, \tag{2.24}$$

has been introduced. The solution to the third-order perturbation equation (2.21) is found in a straightforward manner to be

$$X_n^{(3)} = -\frac{\mathcal{S}}{2}\Sigma_0|A|^4\cot\frac{\omega}{2} + (\mathcal{B} + in\mathcal{S}_1\mathcal{F}\sin\omega)|A|^2A^2e^{2i\omega n}$$

$$+ \frac{\sin\omega}{2}\mathcal{S}_3\Sigma_4A^4e^{4i\omega n} + c.c., \tag{2.25}$$

where

$$\mathcal{B} = \frac{\mathcal{S}_1^2}{2}\Big(\mathcal{S}_2\sin\omega - \mathcal{S}\cot\frac{\omega}{2}\Big)\sin^2\omega - \frac{\mathcal{S}_1^2\mathcal{F}}{\mathcal{S}}\sin\omega\sin 2\omega, \tag{2.26}$$

$$\mathcal{S}_3 = \frac{\mathcal{S}}{\cos\omega - \cos 4\omega}, \qquad \omega \neq \frac{2\pi}{5} + 2k\pi, \qquad \omega \neq \frac{4\pi}{5} + 2k\pi. \tag{2.27}$$

Finally, we retain terms proportional to the fundamental harmonic $e^{i\omega n}$ in the fourth-order perturbation equation, i.e.,

$$\widehat{\mathcal{L}}X_n^{(4)} = \Big(\mathcal{C} - 2in\mathcal{F}^2\sin\omega\Big)|A|^4Ae^{i\omega n} + c.c., \tag{2.28}$$

where

$$\mathcal{C} = -2\mathcal{S}\Big(\mathcal{B} + \frac{\mathcal{S}_1^2\mathcal{S}_2}{4}\sin^3\omega - \frac{\mathcal{S}\Sigma_0}{2}\cot\frac{\omega}{2}\Big)\sin\omega. \tag{2.29}$$

We obtain the secular fourth-order contribution to the fundamental harmonic in the form

$$X_n^{(4)} = \left(in\mathcal{D} - \frac{n^2\mathcal{F}^2}{2} \right) |A|^4 A e^{i\omega n} + c.c., \tag{2.30}$$

where the coefficient $\mathcal{D}$ is defined by

$$\mathcal{D} = -\frac{\mathcal{C} + \mathcal{F}^2 \cos\omega}{2\sin\omega}. \tag{2.31}$$

Close inspection of the naive perturbation solution starting from the second-order result (2.19) shows that secular terms (proportional to n, n^2, etc.) are present. To remove these terms, we define the renormalization transformation $A \to \widetilde{A}(n)$ by collecting all terms proportional to the fundamental harmonic $e^{i\omega n}$. This gives

$$\widetilde{A}(n) = \left[1 + i\epsilon^2 n\mathcal{F}|A|^2 + \epsilon^4 \left(in\mathcal{D} - \frac{n^2\mathcal{F}^2}{2} \right) |A|^4 \right] A. \tag{2.32}$$

Solving perturbatively equation (2.32) for A in terms of $\widetilde{A}(n)$, we obtain

$$A = \left[1 - i\epsilon^2 n\mathcal{F} \left| \widetilde{A}(n) \right|^2 + O\left(\epsilon^3\right) \right] \widetilde{A}(n). \tag{2.33}$$

A discrete version of the RG equation can be defined by considering the difference

$$\widetilde{A}(n+1) - \widetilde{A}(n) = i\epsilon^2 \mathcal{F}|A|^2 A + \epsilon^4 \left(i\mathcal{D} - \frac{\mathcal{F}^2}{2} - n\mathcal{F}^2 \right) |A|^4 A. \tag{2.34}$$

Substituting the expression for A in terms of $\widetilde{A}(n)$ [see equation (2.33)] into the right-hand-side of equation (2.34), we can eliminate the secular terms up to $O(\epsilon^4)$. This gives

$$\widetilde{A}(n+1) = \left[1 + i\epsilon^2 \mathcal{F} \left| \widetilde{A}(n) \right|^2 + \epsilon^4 \left(i\mathcal{D} - \frac{\mathcal{F}^2}{2} \right) \left| \widetilde{A}(n) \right|^4 \right] \widetilde{A}(n). \tag{2.35}$$

This naive RG map does not preserve the symplectic symmetry of the original system and does not have a *constant of the motion*. To recover the symplectic symmetry, we regularize [15] the naive RG map (2.35) by noting that the coefficient in the square brackets multiplying $\widetilde{A}(n)$ can be exponentiated as

$$\widetilde{A}(n+1) = \widetilde{A}(n) \exp\left[i\widetilde{\omega}\left(\left| \widetilde{A}(n) \right| \right) \right], \tag{2.36}$$

where

$$\widetilde{\omega}\left(\left| \widetilde{A}(n) \right| \right) = \epsilon^2 \mathcal{F} \left| \widetilde{A}(n) \right|^2 + \epsilon^4 \mathcal{D} \left| \widetilde{A}(n) \right|^4. \tag{2.37}$$

Although the renormalization procedure described above may seem somewhat artificial, it holds in all orders. By extracting a symplectic implicit map in terms of the real part and the argument (phase) of the renormalized amplitude $\widetilde{A}(n)$, a partial proof (up to fourth order)

of this assertion will be presented in the next paragraph. It is clear now that the regularized RG map (2.36) possesses the obvious integral of motion

$$\left|\widetilde{A}(n+1)\right| = \left|\widetilde{A}(n)\right| = \sqrt{\frac{\mathcal{J}}{2}}. \tag{2.38}$$

It is important to note that the secular terms encountered in the higher harmonics ($e^{2i\omega n}$, $e^{3i\omega n}$, etc.) can be summed to give the renormalized amplitudes, which when expressed in terms of $\widetilde{A}(n)$ do not contain secular terms. This means that once the amplitude of the fundamental harmonic is renormalized, any problems associated with divergences in higher harmonics are being remedied automatically. To demonstrate this, we express the amplitude of the second harmonic as

$$A_2 = \epsilon\Big[\frac{\mathcal{S}_1}{2}\sin\omega + \epsilon^2(\mathcal{B} + in\mathcal{S}_1\mathcal{F}\sin\omega)|A|^2\Big]A^2, \tag{2.39}$$

which by virtue of equation (2.33) acquires the form

$$A_2 = \epsilon\Big[\frac{\mathcal{S}_1}{2}\sin\omega + \epsilon^2\mathcal{B}\Big|\widetilde{A}(n)\Big|^2\Big]\widetilde{A}^2(n). \tag{2.40}$$

By analogy, the amplitude of the third harmonic

$$A_3 = \epsilon^2\Big[\frac{\mathcal{S}_1\mathcal{S}_2}{2}\sin^2\omega + \epsilon^2\Big(\mathcal{B}_3 + \frac{3in}{2}\mathcal{S}_1\mathcal{S}_2\mathcal{F}\sin^2\omega\Big)|A|^2\Big]A^3 \tag{2.41}$$

can also be renormalized. The result is

$$A_3 = \epsilon^2\Big[\frac{\mathcal{S}_1\mathcal{S}_2}{2}\sin^2\omega + \epsilon^2\mathcal{B}_3\Big|\widetilde{A}(n)\Big|^2\Big]\widetilde{A}^3(n). \tag{2.42}$$

Proceeding in a manner similar to above, we can represent the canonical conjugate momentum P_n according to

$$P_n = i\widetilde{B}(n)e^{i\omega n} + c.c. + \text{higher harmonics}, \tag{2.43}$$

where

$$\widetilde{B}(n+1) = \widetilde{B}(n)\exp\Big[i\widetilde{\omega}\Big(\Big|\widetilde{A}(n)\Big|\Big)\Big]. \tag{2.44}$$

Using now the relation (2.4) between the canonical conjugate variables (X_n, P_n), we can express the renormalized amplitude $\widetilde{B}(n)$ in terms of $\widetilde{A}(n)$ as

$$\widetilde{B}(n) = \frac{i\widetilde{A}(n)}{\sin\omega}\Big[e^{-i\left(\omega+\widetilde{\omega}\right)} - \cos\omega\Big]. \tag{2.45}$$

In addition, the sextupole nonlinearity shifts the closed orbit by the constant value (in normalized coordinates)

$$X_{co} = -\frac{\epsilon\mathcal{S}\mathcal{J}}{2}\left[1 + \frac{\epsilon^2}{4}\Sigma_0\mathcal{J} + O\Big(\epsilon^3\Big)\right]\cot\frac{\omega}{2}, \qquad P_{co} = -X_{co}\tan\frac{\omega}{2}, \tag{2.46}$$

which is a common property for all odd multipole nonlinearities.

Neglecting higher harmonics and iterating the regularized RG maps (2.36) and (2.44), the renormalized solution of the Henon map can be expressed as

$$X_n^{(1)} = X_{co} + \sqrt{2\mathcal{J}}\cos\psi(\mathcal{J};n), \tag{2.47}$$

$$P_n^{(1)} = P_{co} + \sqrt{2\mathcal{J}}\Big[\alpha_H^{(1)}(\mathcal{J})\cos\psi(\mathcal{J};n) - \beta_H^{(1)}(\mathcal{J})\sin\psi(\mathcal{J};n)\Big], \tag{2.48}$$

where

$$\psi(\mathcal{J};n) = [\omega + \widetilde{\omega}(\mathcal{J})]n + \widetilde{\phi}, \tag{2.49}$$

$$\alpha_H^{(1)}(\mathcal{J}) = \frac{\cos\omega - \cos[\omega+\widetilde{\omega}(\mathcal{J})]}{\sin\omega}, \qquad \beta_H^{(1)}(\mathcal{J}) = \frac{\sin[\omega+\widetilde{\omega}(\mathcal{J})]}{\sin\omega}. \tag{2.50}$$

It is evident that the integral of motion $\mathcal{J}$ has the form of a *generalized Courant-Snyder invariant* [23], which can be expressed as

$$2\mathcal{J} = \Big(X^{(1)} - X_{co}\Big)^2 + \frac{\Big[P^{(1)} - P_{co} - \alpha_H^{(1)}(\mathcal{J})\Big(X^{(1)} - X_{co}\Big)\Big]^2}{\beta_H^{(1)\mathbf{2}}(\mathcal{J})}. \tag{2.51}$$

It is important to emphasize that equation (2.51) represents a transcendental equation for the invariant $\mathcal{J}$ as a function of the canonical variables (X, P), because the coefficients α_H and β_H depend on $\mathcal{J}$. Note also that the sextupole nonlinearity gives rise to a nonlinear tune shift $\widetilde{\omega}$, leading to the distortion of the invariant curves [circles in normalized phase space (X, P)][†] even in an approximation where only the contribution of the first harmonic is taken into account. Further distortions of the phase-space trajectories are introduced by higher harmonics.

Taking into account all harmonics up to the fifth harmonic, we can express the renormalized fourth-order solution of the *Henon* map in the form

$$X_n = X_n^{(1)} + \sum_{M=2}^{5} \mathcal{X}_M \cos M\psi(\mathcal{J};n), \tag{2.52}$$

$$P_n = P_n^{(1)} + \sum_{M=2}^{5} \mathcal{X}_M\Big[\alpha_H^{(M)}\cos M\psi(\mathcal{J};n) - \beta_H^{(M)}\sin M\psi(\mathcal{J};n)\Big]. \tag{2.53}$$

The amplitudes $\mathcal{X}_M$ of the various harmonics are given by the expressions

$$\mathcal{X}_2 = \frac{\epsilon\mathcal{J}}{2}\Big(\mathcal{S}_1\sin\omega + \epsilon^2\mathcal{B}\mathcal{J}\Big), \qquad \mathcal{X}_4 = \frac{1}{4}\epsilon^3\mathcal{S}_3\Sigma_4\mathcal{J}^2\sin\omega, \tag{2.54}$$

$$\mathcal{X}_3 = \frac{\epsilon^2\mathcal{J}\sqrt{\mathcal{J}}}{2\sqrt{2}}\Big(\mathcal{S}_1\mathcal{S}_2\sin^2\omega + \epsilon^2\mathcal{B}_3\mathcal{J}\Big), \qquad \mathcal{X}_5 = \frac{1}{2\sqrt{2}}\epsilon^4\mathcal{C}_5\mathcal{J}^2\sqrt{\mathcal{J}}. \tag{2.55}$$

Furthermore, similar to equation (2.50), the generalized $\alpha_H^{(M)}$ and $\beta_H^{(M)}$ functions can be expressed as

$$\alpha_H^{(M)}(\mathcal{J}) = \frac{\cos\omega - \cos M[\omega+\widetilde{\omega}(\mathcal{J})]}{\sin\omega}, \qquad \beta_H^{(M)}(\mathcal{J}) = \frac{\sin M[\omega+\widetilde{\omega}(\mathcal{J})]}{\sin\omega}. \tag{2.56}$$

[†]Note that $\alpha_H = 0$ and $\beta_H = 1$ for $\widetilde{\omega} = 0$.

3 Resonance Structure of the Henon Map

The solution to the first-order perturbation equation (2.13) was obtained in the form (2.14) assuming that the unperturbed betatron tune ν is far from the third-order resonance $3\nu = 1$. It is important to study the properties of the *Henon* map near a nonlinear resonance by means of the RG method. In what follows, we demonstrate how the RG reduction of the *Henon* map works near the one-third resonance. A similar procedure can be performed near all other resonances.

Let us expand ω according to

$$\omega = \omega_0 + \epsilon\delta_1 + \epsilon^2\delta_2 + \dots, \qquad \omega_0 = \frac{2\pi}{3}. \tag{3.1}$$

Equation (2.5) can then be expressed in alternate form

$$\widehat{\mathcal{L}}_0 X_n = X_{n+1} - 2X_n\cos\omega_0 + X_{n-1} = 2X_n(\cos\omega - \cos\omega_0) - \epsilon\mathcal{S}X_n^2\sin\omega. \tag{3.2}$$

The perturbation expansion (2.6), when substituted into equation (3.2), yields the perturbation equations

$$\widehat{\mathcal{L}}_0 X_n^{(0)} = 0, \tag{3.3}$$

$$\widehat{\mathcal{L}}_0 X_n^{(1)} = -\frac{\sqrt{3}}{2}\Big(2\delta_1 X_n^{(0)} + \mathcal{S}X_n^{(0)\mathbf{2}}\Big), \tag{3.4}$$

$$\widehat{\mathcal{L}}_0 X_n^{(2)} = -\sqrt{3}\delta_1 X_n^{(1)} + \left(\frac{\delta_1^2}{2} - \sqrt{3}\delta_2\right)X_n^{(0)} + \mathcal{S}\left(\frac{\delta_1}{2}X_n^{(0)\mathbf{2}} - \sqrt{3}X_n^{(0)}X_n^{(1)}\right). \tag{3.5}$$

Noting that $2\omega_0 = 2\pi - \omega_0$, equations (3.3)-(3.5) can be solved, yielding the result

$$X_n^{(0)} = Ae^{i\omega_0 n} + c.c., \qquad P_n^{(0)} = iAe^{i\omega_0 n} + c.c., \tag{3.6}$$

$$X_n^{(1)} = -\frac{\mathcal{S}\sqrt{3}}{3}|A|^2 + in\mathcal{G}(A, A^*)e^{i\omega_0 n} + c.c., \tag{3.7}$$

$$X_n^{(2)} = \mathcal{A} + in\mathcal{B} + \Big(in\mathcal{C} + n^2\mathcal{D}\Big)e^{i\omega_0 n} + c.c., \tag{3.8}$$

where

$$\mathcal{G}(A, A^*) = \delta_1 A + \frac{\mathcal{S}}{2}A^{*\mathbf{2}}, \tag{3.9}$$

$$\mathcal{A} = \frac{2\delta_1}{3}\mathcal{S}|A|^2, \qquad \mathcal{B} = \frac{\sqrt{3}\mathcal{S}}{3}(\mathcal{G}^*A - \mathcal{G}A^*), \tag{3.10}$$

$$\mathcal{D} = \frac{1}{2}(-\delta_1\mathcal{G} + \mathcal{S}\mathcal{G}^*A^*), \qquad \mathcal{C} = -\frac{\Sigma + \mathcal{D}}{\sqrt{3}}, \tag{3.11}$$

$$\Sigma = \left(\frac{\delta_1^2}{2} - \sqrt{3}\delta_2\right)A + \frac{\delta_1\mathcal{S}}{2}A^{*\mathbf{2}} + \mathcal{S}^2|A|^2A. \tag{3.12}$$

Proceeding as before, we define the renormalized amplitude by

$$\widetilde{A}(n) = A + i\epsilon n\mathcal{G} + \epsilon^2\Big(in\mathcal{C} + n^2\mathcal{D}\Big). \tag{3.13}$$

Taking into account the expression

$$A = \widetilde{A} - i\epsilon n\mathcal{G}\Big(\widetilde{A}, \widetilde{A}^*\Big) + O\Big(\epsilon^2\Big), \tag{3.14}$$

which relates the amplitude A to the renormalized amplitude $\widetilde{A}(n)$, we obtain the renormalized resonant map

$$\widetilde{A}(n+1) = \widetilde{A}(n) + i\epsilon\widetilde{\mathcal{G}}(n) + \epsilon^2\Big[i\widetilde{\mathcal{C}}(n) + \widetilde{\mathcal{D}}(n)\Big], \tag{3.15}$$

where

$$\widetilde{\Lambda}(n) = \Lambda\Big[\widetilde{A}(n), \widetilde{A}^*(n)\Big], \tag{3.16}$$

and Λ represents $\mathcal{C}$, $\mathcal{D}$ or $\mathcal{G}$.

It is important to note that the resonant shift in the closed orbit is automatically renormalized, once the renormalization transformation $A \to \widetilde{A}(n)$ has been performed. The result is

$$X_{co}(n) = \frac{\epsilon\mathcal{S}}{3}\Big[-\sqrt{3} + 2\epsilon\delta_1 + O\Big(\epsilon^2\Big)\Big]\Big|\widetilde{A}(n)\Big|^2. \tag{3.17}$$

Note that the closed orbit can be corrected up to third order (in the sextupole strength $\mathcal{S}$) by choosing the first-order resonance detuning δ_1 to be $\delta_1 = \sqrt{3}/2$. In terms of betatron tune, this implies

$$\Delta\nu = \frac{\sqrt{3}}{4\pi}. \tag{3.18}$$

Since the naive RG map (3.15) does not preserve the symplectic structure of the original Henon map, an important step at this point consists of constructing a symplectic map in appropriate variables equivalent to (3.15). Unfortunately, the regularization procedure described in the previous paragraph cannot be applied to the map (3.15). The reason is that in the resonant case $\Big|\widetilde{A}(n)\Big|$ is no longer an integral of motion. An alternative way to overcome this difficulty is to represent $\widetilde{A}(n)$ as

$$\widetilde{A}(n) = \sqrt{\mathcal{J}_n}e^{i\varphi_n}, \tag{3.19}$$

and attempt to find an (implicit) map in terms of the new variables $(\varphi_n, \mathcal{J}_n)$ of the form

$$\varphi_{n+1} = \varphi_n + g(\mathcal{J}_{n+1}, \varphi_n), \qquad \mathcal{J}_{n+1} = \mathcal{J}_n + f(\mathcal{J}_{n+1}, \varphi_n). \tag{3.20}$$

Expanding the unknown functions f and g in a perturbation series

$$f = \sum_{k=1}^{\infty}\epsilon^k f_k, \qquad g = \sum_{k=1}^{\infty}\epsilon^k g_k, \tag{3.21}$$

and substituting equation (3.19) into equation (3.15), we can determine f and g up to second order. We obtain

$$f_1(\varphi, \mathcal{J}) = \mathcal{S}\mathcal{J}^{3/2}\sin 3\varphi, \qquad g_1(\varphi, \mathcal{J}) = \delta_1 + \frac{\mathcal{S}}{2}\sqrt{\mathcal{J}}\cos 3\varphi, \tag{3.22}$$

$$f_2(\varphi,\mathcal{J}) = 3\delta_1\mathcal{S}\mathcal{J}^{3/2}\cos 3\varphi - \frac{\delta_1\mathcal{S}\sqrt{3}}{2}\mathcal{J}^{3/2}\sin 3\varphi + \frac{3\mathcal{S}^2}{4}\mathcal{J}^2\cos 6\varphi, \tag{3.23}$$

$$\begin{aligned} g_2(\varphi,\mathcal{J}) = \delta_2 - \frac{5\mathcal{S}^2\sqrt{3}}{12}\mathcal{J} - \frac{3\delta_1\mathcal{S}}{4}\sqrt{\mathcal{J}}\sin 3\varphi \\ - \frac{\delta_1\mathcal{S}\sqrt{3}}{4}\sqrt{\mathcal{J}}\cos 3\varphi - \frac{\mathcal{S}^2}{4}\mathcal{J}\sin 6\varphi, \end{aligned} \tag{3.24}$$

The map (3.20) is symplectic provided the condition

$$\frac{\partial g}{\partial \varphi_n} + \frac{\partial f}{\partial \mathcal{J}_{n+1}} = 0 \tag{3.25}$$

holds. To verify equation (3.25), we evaluate the determinant of its Jacobian

$$\det\left(\widehat{\mathcal{J}}_{\mathcal{M}}\right) = \det\begin{pmatrix} 1 + g_{\varphi_n} + g_{\mathcal{J}_{n+1}}\dfrac{\partial \mathcal{J}_{n+1}}{\partial \varphi_n} & g_{\mathcal{J}_{n+1}}\dfrac{\partial \mathcal{J}_{n+1}}{\partial \mathcal{J}_n} \\ f_{\varphi_n} + f_{\mathcal{J}_{n+1}}\dfrac{\partial \mathcal{J}_{n+1}}{\partial \varphi_n} & 1 + f_{\mathcal{J}_{n+1}}\dfrac{\partial \mathcal{J}_{n+1}}{\partial \varphi_n} \end{pmatrix}, \tag{3.26}$$

where subscripts denote differentiation with respect to the variables indicated. Taking into account

$$\frac{\partial \mathcal{J}_{n+1}}{\partial \varphi_n} = f_{\varphi_n} + f_{\mathcal{J}_{n+1}}\frac{\partial \mathcal{J}_{n+1}}{\partial \varphi_n} \quad \Longrightarrow \quad \frac{\partial \mathcal{J}_{n+1}}{\partial \varphi_n} = \frac{f_{\varphi_n}}{1 - f_{\mathcal{J}_{n+1}}}, \tag{3.27}$$

$$\frac{\partial \mathcal{J}_{n+1}}{\partial \mathcal{J}_n} = 1 + f_{\mathcal{J}_{n+1}}\frac{\partial \mathcal{J}_{n+1}}{\partial \mathcal{J}_n} \quad \Longrightarrow \quad \frac{\partial \mathcal{J}_{n+1}}{\partial \mathcal{J}_n} = \frac{1}{1 - f_{\mathcal{J}_{n+1}}}, \tag{3.28}$$

we obtain

$$\det\left(\widehat{\mathcal{J}}_{\mathcal{M}}\right) = \frac{1 + g_{\varphi_n}}{1 - f_{\mathcal{J}_{n+1}}}. \tag{3.29}$$

The requirement that $\det\left(\widehat{\mathcal{J}}_{\mathcal{M}}\right) = 1$ leads to the condition (3.25). It is straightforward to verify that f and g as given by equations (3.22) - (3.24) satisfy equation (3.25).

The representation (3.19) of the renormalized amplitude $\widetilde{A}(n)$ together with (3.20) can be used as an alternate way to obtain the exponential form (2.36) of the RG map (2.35). The expansions

$$f = \sum_{k=1}^{\infty}\epsilon^{2k} f_{2k}, \qquad\qquad g = \sum_{k=1}^{\infty}\epsilon^{2k} g_{2k}, \tag{3.30}$$

when substituted into equation (2.35), after some straightforward algebra lead to the result

$$f_2(\varphi,\mathcal{J}) \equiv 0, \qquad\qquad f_4(\varphi,\mathcal{J}) \equiv 0, \tag{3.31}$$

$$g_2(\varphi,\mathcal{J}) = \mathcal{F}\mathcal{J}, \qquad\qquad g_4(\varphi,\mathcal{J}) = \mathcal{D}\mathcal{J}^2. \tag{3.32}$$

Thus, we obtain the symplectic implicit map

$$\varphi_{n+1} = \varphi_n + \epsilon^2\mathcal{F}\mathcal{J}_{n+1} + \epsilon^4\mathcal{D}\mathcal{J}_{n+1}^2, \qquad\qquad \mathcal{J}_{n+1} = \mathcal{J}_n, \tag{3.33}$$

which is the RG map (2.36) written for the real part and the argument of the amplitude $\widetilde{A}(n)$.

4 Numerical Results

In this section we present illustrative numerical results revealing the stability properties of the Henon map. We use the analytical renormalized solution expressed by equations (2.52) - (2.56) to construct the phase portrait of the Henon map near the third-order resonance with $\nu = 0.323$ (also $\nu = 0.34525$), near the fourth-order resonance with $\nu = 0.24$, and near the fifth-order resonance with $\nu = 0.19$. All calculations are performed for a relatively large value of the sextupole strength corresponding to $\mathcal{S} = 0.1$.

In Figure 1 the phase portrait of the Henon map near the third-order resonance with $\nu = 0.323$ is depicted. It shows the stability region and the invariant curves for different values of the modulus squared of the renormalized amplitude $\widetilde{A}$ [see equation (2.38)]. As the value of the invariant $\mathcal{J}$ increases, it reaches a value $\mathcal{J}_{max}$ above which the phase trajectories begin to intersect. This is due to the fact that the perturbation renormalization technique, valid for unperturbed betatron tunes sufficiently far from resonances, does not work well in this region, and the reduction procedure near resonances developed in section 3 should be employed. However, the quantity $\mathcal{J}_{max}$ is closely related to the *dynamic aperture*. For the case where $\nu = 0.323$ it is approximately $\mathcal{J}_{max} = 3.85$. Figure 2 represents the phase portrait of the Henon map for $\nu = 0.34525$. The value of $\mathcal{J}_{max}$ is the same as in the case where $\nu = 0.323$.

Figures 3 and 4 show the phase portrait of the Henon map near the fourth-order and the fifth-order resonances where $\nu = 0.24$ and $\nu = 0.19$, respectively. The dynamic aperture in the case of the fourth-order resonance is approximately $\mathcal{J}_{max} = 19.01$, while in the case of the fifth-order resonance it is $\mathcal{J}_{max} = 28.5$.

5 Conclusions

While the renormalization group method is well established in applications to continuous dynamical systems, the present paper demonstrates that the renormalization group method can also be applied successfully to study discrete dynamical systems. As a particular example, we considered the Henon map as applied to describe the transverse betatron oscillations in a cyclic accelerator or storage ring possessing a FODO-cell structure with a single thin sextupole. The basic equations and Henon transfer map used in the present analysis were summarized in section 1, and in section 2 a powerful renormalization group technique was developed that is valid correct to fourth order in the perturbation amplitude. A technique for resolving the resonance structure of the Henon map was discussed in section 3, and in section 4 illustrative numerical results were presented. To the best of our knowledge, the present calculation represents the first successful application of a powerful renormalization group method to the study of discrete dynamical systems in a unified manner. In section 3 it was shown that the renormalization group map can be further expressed in terms of an implicit symplectic map in both cases, far from and close to resonances. Further applications to discrete dynamical systems will include generic polynomial transfer maps, the standard Chirikov-Taylor map, etc.

Acknowledgments

It is a pleasure to thank Prof. Alex Chao and Prof. Y. Oono for careful reading of the manuscript and for making valuable comments and suggestions. This research was supported by the U.S. Department of Energy.

References

[1] A.W. Chao, *"Physics of Collective Beam Instabilities in High Energy Accelerators"* (John Wiley & Sons, New York, 1993).

[2] D.A. Edwards and M.J. Syphers, *"An Introduction to the Physics of High Energy Accelerators"* (John Wiley & Sons, New York, 1993).

[3] R.C. Davidson and H. Qin, *"Physics of Intense Charged Particle Beams in High Energy Accelerators"* (World Scientific, Singapore, 2001).

[4] P.J. Bryant and K. Johnsen, *"Principles of Circular Accelerators and Storage Rings"* (Cambridge University Press, Cambridge, 1993).

[5] S. Chattopadhyay *et al* (ed), *Nonlinear Dynamics in Particle Accelerators: Theory and Experiments (Arcidosso, 1994) (AIP Conf. Proc. Vol. 344)* (American Institute of Physics, New York 1995).

[6] S. Chattopadhyay *et al* (ed), *Nonlinear and Collective Phenomena in Beam Physics (Arcidosso, 1996) (AIP Conf. Proc. Vol. 395)* (American Institute of Physics, New York 1997).

[7] A.J. Lichtenberg and M.A. Lieberman, *"Regular and Stochastic Motion"* (Springer, Berlin, 1983).

[8] A.H. Nayfeh, *"Introduction to Perturbation Techniques"* (John Wiley & Sons, New York, 1981).

[9] A.J. Dragt, *Physics of High Energy Particle accelerators. Lectures on Nonlinear Orbit Dynamics (Fermilab Summer School, 1981) (AIP Conf. Proc. Vol. 87)*, R.A. Carrigan *et al* (ed) (American Institute of Physics, New York 1982).

[10] G.E.O. Giacaglia, *"Perturbation Methods in Nonlinear Systems" (Appl. Math. Sci. No 8)* (Springer, Berlin, 1972).

[11] J.R. Cary, *Phys. Rep.* **79** 129 (1981).

[12] L.-Y. Chen, N. Goldenfeld and Y. Oono, *Phys. Rev.* E**54** 376 (1996).

[13] K. Nozaki and Y. Oono, *Phys. Rev.* E**63** 046101-1 (2001).

[14] S.-I. Ei, K. Fujii and T. Kunihiro, *Ann. Phys., NY* **280** 236 (2000).

[15] S.-I. Goto and K. Nozaki, *J. Phys. Soc. Japan* **70** 49 (2001).

[16] T. Kunihiro and J. Matsukidaira, *Phys. Rev.* E**57** 4817 (1998).

[17] V.I. Arnold and A. Avez, *"Ergodic Problems of Classical Mechanics"* (Benjamin, New York, 1968).

[18] R.W. Zwanzig, *Lectures in Theoretical Physics* Vol. 3, W.E. Brittin (ed) (John Wiley & Sons, New York 1961).

[19] S.I. Tzenov, *New J. Phys.* **4** 6.1 (2002).

[20] M. Henon, *Quart. J. Appl. Math.* **27** 291 (1969).

[21] M. Henon, *Comm. Math. Phys.* **50** 69 (1976).

[22] S.I. Tzenov, *"Contemporary Accelerator Physics"* (World Scientific, Singapore, 2003).

[23] E.D. Courant and H.S. Snyder, *Ann. Phys., NY* **3** 1 (1958).

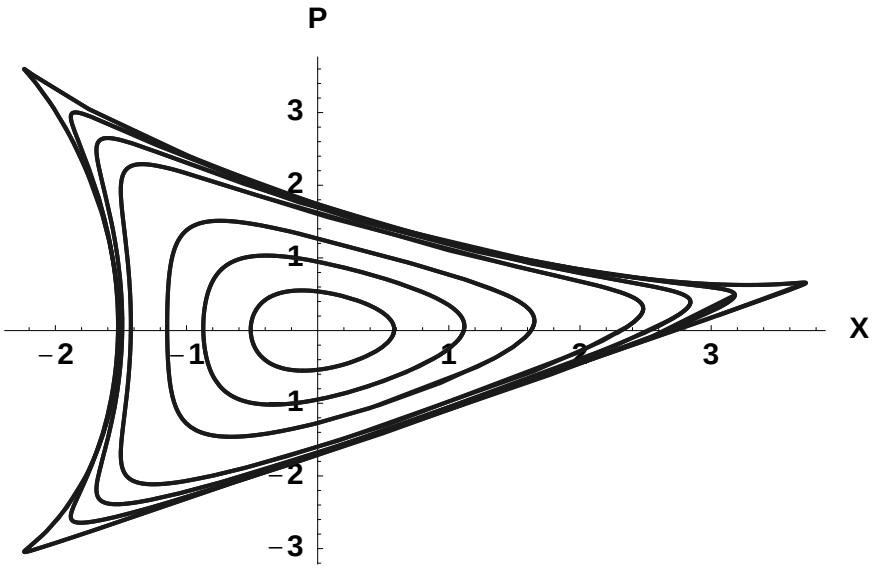


Figure 1: Phase portrait of the Henon map obtained from equations (2.52) - (2.56) near the third-order resonance with $\nu = 0.323$. Here, $\mathcal{J}$ takes values ranging from $\mathcal{J} = 0.15$ (inner contour) to $\mathcal{J} = \mathcal{J}_{max} = 3.85$ (outer contour).

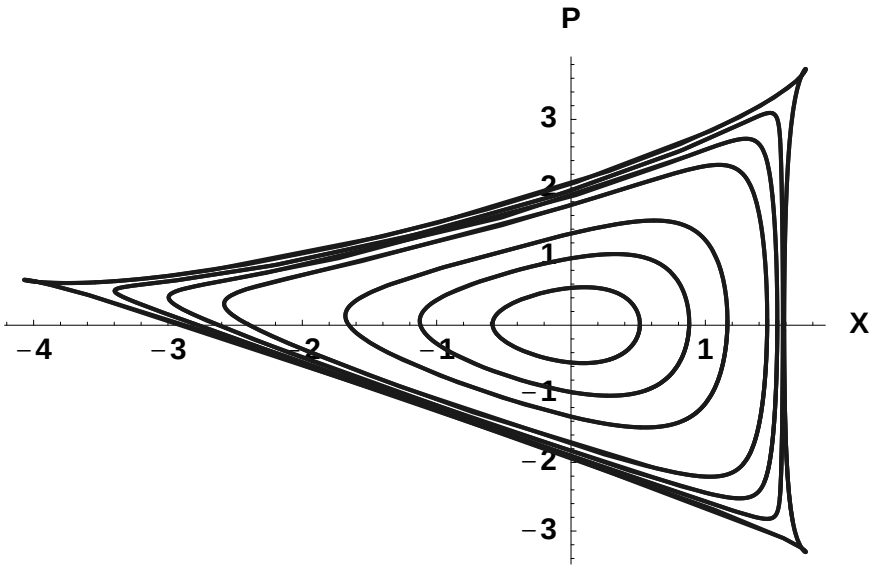


Figure 2: Phase portrait of the Henon map obtained from equations (2.52) - (2.56) near the third-order resonance with $\nu = 0.34525$. Here, $\mathcal{J}$ takes values ranging from $\mathcal{J} = 0.15$ (inner contour) to $\mathcal{J} = \mathcal{J}_{max} = 3.85$ (outer contour).

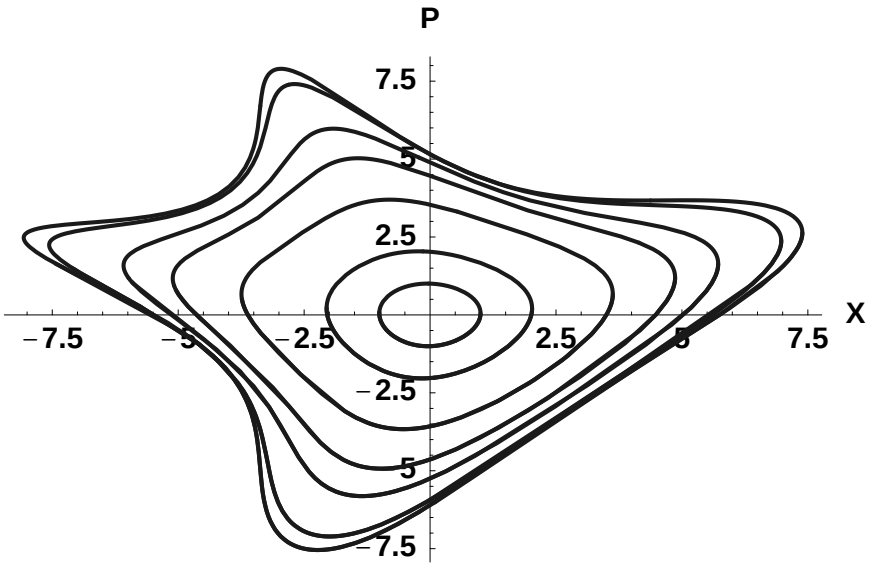


Figure 3: Phase portrait of the Henon map obtained from equations (2.52) - (2.56) near the fourth-order resonance with $\nu = 0.24$. Here, $\mathcal{J}$ takes values ranging from $\mathcal{J} = 0.5$ (inner contour) to $\mathcal{J} = \mathcal{J}_{max} = 19.01$ (outer contour).

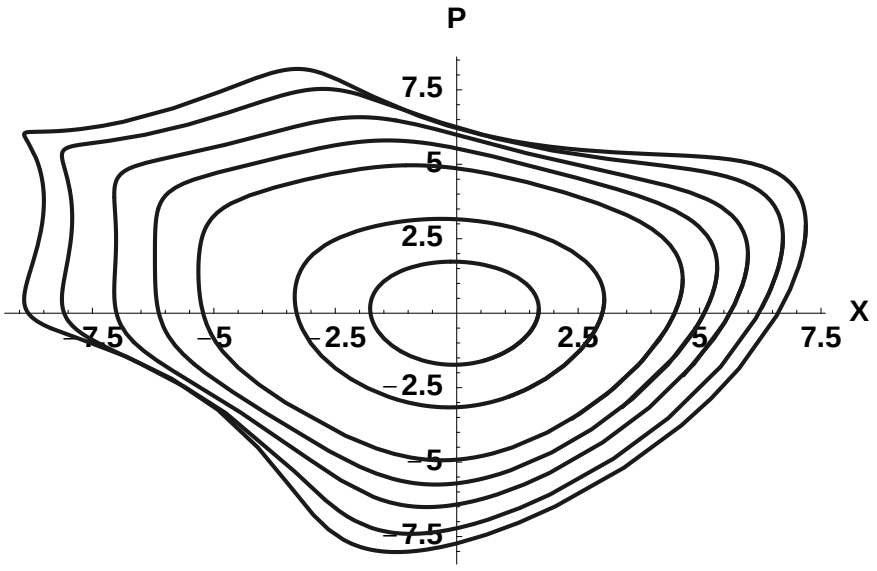


Figure 4: Phase portrait of the Henon map obtained from equations (2.52) - (2.56) near the fifth-order resonance with $\nu = 0.19$. Here, $\mathcal{J}$ takes values ranging from $\mathcal{J} = 1.5$ (inner contour) to $\mathcal{J} = \mathcal{J}_{max} = 28.5$ (outer contour).